A Multi-algorithmic Colour Iris Recognition System

Petru Radu, Konstantinos Sirlantzis, Gareth Howells,
Sanaul Hoque, and Farzin Deravi

School of Engineering and Digital Arts,
University of Kent, Canterbury, U.K
{pr95,k.sirlantzis,w.g.j.howells,s.hoque,f.deravi}@kent.ac.uk

Abstract. The reported accuracies of iris recognition systems are generally higher on near infrared images than on colour RGB images. To increase a colour iris recognition system's performance, a possible solution is a multi-algorithmic approach with an appropriate fusion mechanism. In the present work, this approach is investigated by fusing three algorithms at the score level to enhance the performance of a colour iris recognition system. The contribution of this paper consists of proposing 2 novel feature extraction methods for colour iris images, one based on a 3-bit encoder of the 8 neighborhood and the other one based on gray level co-occurrence matrix. The third algorithm employed uses the classical Gabor filters and phase encoding for feature extraction. A weighted average is used as a matching score fusion. The efficiency of the proposed iris recognition system is demonstrated on UBIRISv1 dataset.

1 Introduction

Iris recognition has become an emerging research topic due to its rich texture with a high number of degrees of freedom [1], which has allowed researchers to develop a large variety of iris authentication algorithms. Although the performance of the iris recognition algorithms is high [2, 3], they require a large amount of constraints on the user due to the fact that near infrared illumination is necessary for good quality images and a reliable operation.

The majority of iris recognition systems published in the literature have only been benchmarked on near infrared images, leaving a question mark on whether these algorithms can perform on colour iris images with a comparable accuracy. The pioneering iris recognition system proposed in [1], which uses phase based coding and binary features extracted from near infrared images is deployed in most of the commercial and military iris recognition devices currently available. This fact led to the formation of large iris databases which contain images acquired under near infrared illumination.

The United States National Institute of Standards and Technology (NIST) [4] conducted a series of iris recognition competitions [5], where the submitted algorithms were tested on large scale databases containing near infrared iris images. These competitions allowed the creation of an ISO standard for near infrared iris images [6], which will promote the interoperability between various iris recognition acquisition devices and authentication algorithms. Generally the near infrared iris image data

V.E. Balas et al. (Eds.): Soft Computing Applications, AISC 195, pp. 45–56.
springerlink.com

standard specifies the thresholds for different iris image quality measures, which from a practical point of view are translated into how large the constraints on the user have to be.

For iris images acquired in visible spectrum there hasn't been created a standard yet, but over the past several years advances have been made in colour iris recognition. However, the accuracies obtained in visible spectrum are not yet comparable to those obtained under near infrared illumination [7]. The practicability of a colour iris recognition system is considerably increased when compared to a near infrared iris recognition system because the constraints on the user are significantly relaxed. One of the pioneers of iris recognition in visible spectrum is Hugo Proenca, who organized a colour iris recognition competition called Noisy Iris Challenge Evaluation (NICE). It took place in 2 parts: part1 assessed only the segmentation of a subset of UBIRISv2 [8] dataset and in part 2 the classification algorithms were assessed on the same images. Proenca et al analyzed the results of the second part of NICE competition in [7], where they reported that by employing a multi-algorithmic approach between the top 5 ranked algorithms, the accuracy of the system increases significantly.

In this paper we employ a multi-algorithmic approach to enhance a colour iris recognition systems' accuracy, motivated by the results reported in [7]. We use three iris recognition algorithms, two proposed by us in the present paper and one is the classical method proposed in [1].

The main novelty of the present work consists of 2 iris feature extraction methods. The first one uses the gray levels of the 8 neighborhood of a pixel from the iris texture and the second one uses the gray level co-occurrence matrices (GLCM) of the iris texture, calculated for 8 directions. Also, we propose a transformation of the match scores of the iris recognition systems which enhances the separation between authentic and impostor score distributions. Further, we analyze how the system performs when only a small number of pixels around the pupil are unwrapped compared to the case when a large number of pixels around the pupil are used to form the unwrapped image.

The remainder of the paper is organized as follows: in Section 2, the component algorithms of the multi-algorithm iris recognition systems are detailed. In Section 3 the separation enhancement method between authentic and impostor score distributions is presented. The experimental results are reported in Section 4 and conclusions are given in Section 5.

2 Proposed Multi-algorithmic Iris Recognition System

In Fig. 1 the block diagram of the proposed multi-algorithmic iris recognition system is presented. As may be observed, the system only uses the red channel to extract the information from the iris texture. The red channel has the closest wavelength to the near infrared domain and yields the best accuracy from the RGB colour space, as reported in [9].

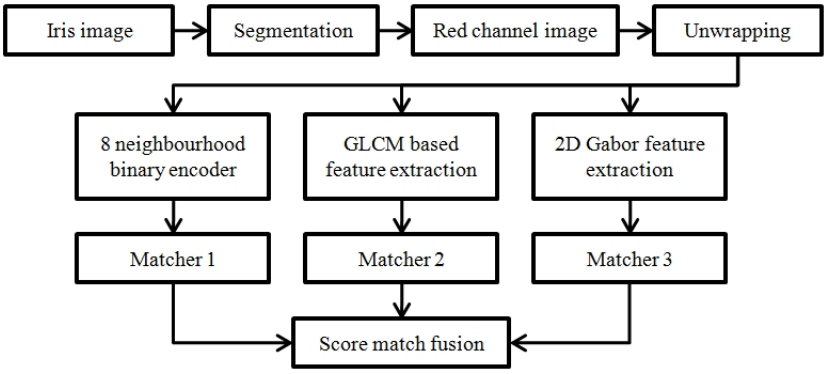

Fig. 1. Multi-algorithmic iris recognition system architecture

2.1 Preprocessing

An iris recognition system consists of five main stages: acquisition, segmentation, normalization, feature extraction and matching. For segmentation, the algorithm proposed in [10] was employed. In this work, we benchmarked the multi-algorithmic system on images from UBIRISv1 [11], Session 1 dataset. The segmentation accuracy on these images was approximately 95%. The remaining 5% were manually segmented, as they contain strong occlusions or other noise factors which make the segmentation difficult.

The unwrapping was done using the rubber sheet model proposed in [1]. To avoid including the eyelashes in the unwrapped image, the circle sector defined between -45^o and +45^o of vertical axis was not considered. The unwrapped image dimension initially is 120 by 50 pixels for the 8 neighborhood binary encoder and the classical phase based feature extraction and 360 by pixels 50 for the GLCM based system. Then, 100 pixels are considered around the pupil and the resulting unwrapped image dimension is 120 by 100 pixels and 360 by 100 pixels respectively.

As an efficient image enhancement was reported in [12] to be the second time consuming task from an iris recognition system after segmentation, our system does not employ any image enhancement techniques.

2.2 8-Neighborhood Binary Encoder

The pixel relationships are the basis of the least computationally demanding texture analysis techniques, as there is no filtering operation necessary. By using the 8 neighborhood of a pixel, we propose an iris feature extraction method which is computationally efficient and is therefore suitable to be implemented on mobile or embedded devices.

The working principle of the proposed feature extraction method is a simple, yet effective one: the 8 positions of the 8-neighborhood of a pixel may be encoded on 3 bits, as shown in Fig. 2. When the center pixel is immediately near its neighbors, we

have an offset of 1, but the offset may be higher. Considering the values of the 8 neighbors of a pixel, the 3 bits corresponding to that pixel are the binary code corresponding to the position of the highest intensity value of the 8 neighbor pixels.

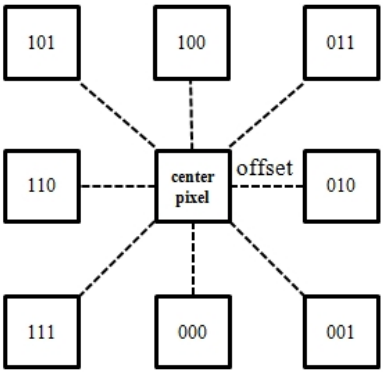

Fig. 2. Binary encoding of 8 neighborhood of a pixel

Additionally to encoding the position of the maximum pixel value of the 8-neighborhood, the value of the center pixel is compared to the mean of the 8-neighborhood. If the center pixel has a value smaller than the average, a logical 0 is concatenated to the 3 bits corresponding to the position of the maximum neighbor, otherwise a logical 1 is concatenated.

The 8-neighborhood does not have necessarily to be considered for every other pixel, it may be considered with a step for the horizontal scan and one for the vertical scan. In this way this feature extraction method becomes even more computationally efficient. We investigated how the performance varies with the step size via a direct search. As a matching algorithm, the Hamming distance is used [1].

The three parameters of this feature extraction method are the offset, the horizontal scanning step and the vertical scanning step. We found these parameters empirically, by taking the first 40 classes from UBIRISv1 [11] Session 1 dataset and computing the decidability index [1], which is a measure of the separation between the authentic and impostor score distributions. We found that the maximum decidability index was obtained for an offset of 7 pixels, a horizontal step of 1 pixel and a vertical step of 5 pixels. The resulting feature size is 3392 bits for the 120 by 50 pixels unwrapped image and 7632 bits for the 120 by 100 pixels image.

2.3 Co-occurrence Matrix Based Features

The co-occurrence matrix C for a 8-bit gray level image *I* is a 256 by 256 matrix which contains on row i and column j the counts of the number of pixels pairs with the intensity values i and j, which are separated by an offset and are at a relative inclination [13]:

$$C_{i,j=}\sum_{x=1}^{256}\sum_{y=1}^{256}\left(I_{x,y}=i\right)\wedge\left(I_{x',y'}=j\right) \tag{1}$$

where x' and y' are the offsets given by the distance d and inclination θ:

$$\begin{cases}x'=x+d\cos\theta\\y'=y+d\sin\theta\end{cases} \tag{2}$$

The GLCM is symmetrical and if it has higher values around the main diagonal, it means that the image contrast is low. In the proposed feature extraction method, 8 co-occurrence non-symmetrical matrices were computed for an unwrapped iris image, corresponding to the directions given by the 8-neighborhood. A fused GLCM was obtained by averaging the 8 initial GLCM.

As the iris texture generally does not have high contrast, the higher values of the fused GLCM were concentrated around the main diagonal. The presence of noises such as eyelashes or reflections in the unwrapped iris image will be observed in high values in corner regions of the GLCM. From the original fused GLCM we only keep the part of the matrix with rows and columns indexes between 75 and 135. Therefore, the feature size will be $(135\text{-}75+1)^2 = 3721$ integer positive values. The indexes 75 and 135 were determined empirically with the criterion of maximizing the decidability index for 40 classes from UBIRISv1 dataset, Session 1, while keeping a manageable feature size of 3621 bytes. The larger the amount of data from the original GLCM is used, the higher the accuracy of the system will be, but the tradeoff is a higher computational demand and a larger template size.

From the selected 61 by 61 pixels matrix, we consider 20 vectors parallel and above the main diagonal and 20 vectors parallel and below the main diagonal. The main diagonal was not considered because it provides information about the pixels with the same intensity level. Let us denote the 20 vectors above the diagonal with v_1, …, v_{20} and the 20 vectors below the main diagonal v_{-1}, …, v_{-20}. In the matching phase, initially the Euclidian distances are computed between the corresponding vectors extracted from the probe and gallery images. As two initial scores, the means of the square roots of the Euclidean distances of the vectors above and below the main diagonal are computed using equations (3). The square root was used as a non-linear transformation to make the authentic and impostor score distributions narrower.

$$\begin{cases}\mathrm{M1}=\dfrac{1}{20}\displaystyle\sum_{i=1}^{20}\sqrt{\left\|v_i^{gallery},v_i^{probe}\right\|}\\[2ex]\mathrm{m2}=\dfrac{1}{20}\displaystyle\sum_{i=-20}^{-1}\sqrt{\left\|v_i^{gallery},v_i^{probe}\right\|}\end{cases} \tag{3}$$

The two means from equations (3) are used to compute the intermediate scores from equations (4). The hyperbolic tangent function is used to normalize the scores between 0 and 1. Hyperbolic tangent function takes values between 0 and 1 for positive

arguments and maps all its arguments which are above 2.5 very close or equal to 1. The argument of hyperbolic tangent was used to bring the impostors scores above the value of 2.5 and the authentic scores as small as possible.

$$\begin{cases} \text{dist1} = \tanh\left(\log\dfrac{20}{1+e^{m1}}\right)^6 \\ \text{dist2} = \tanh\left(\log\dfrac{20}{1+e^{m2}}\right)^6 \end{cases} \tag{4}$$

The final co-occurrence matrix score (CMS) is obtained using equation (5) to fuse dist1 and dist2. dist1 and dist2 are below 1, and the product dist1*dist2 will be close to 0 for authentics and much larger for impostors. The absolute value of the base 2 logarithm of a number which is below 0.15 for example is above 2.5, while the absolute value of the base 2 logarithm of a number which is above 0.6 is below 0.6.

$$CMS = 1 - \tanh|\log_2(\text{dist1} * \text{dist2})| \tag{5}$$

2.4 Classical Phase-Based Feature Extraction

This method employs the classical 2D Gabor filters [1] to extract the information from the iris texture. The features are binary strings extracted using one set of parameters of the 2D Gabor filters. For each pixel of the unwrapped image, 2 bits of information are stored. We observed that if the 2 bits are extracted from every other pixel, the drop in performance is negligible.

The feature size is 3000 bits for the 120 by 50 pixels unwrapped iris image and 6000 bits for the 120 by 100 pixels image. For matching, the classical Hamming distance was used.

The issue of rotation is addressed by shifting one binary string 4 bits to the left and 4 bits to the right and the minimum Hamming distance out of the 9 computations is stored. The same method was applied to compensate for rotation of the features extracted using the 8-neighborhood binary encoder. The features extracted using GLCM are rotational invariant.

3 Enhancing the Authentic and Impostor Distributions

In any iris recognition system it is desirable to have a decidability index [1] between impostor and authentic score distributions as large as possible. A classical iris recognition system has most of the authentic scores concentrated in the range [0;0.2], while most of the impostor scores are above 0.4 [14-16].

In this paper we propose a transformation of the scores of an iris recognition system with the properties mentioned above by using equation (6). We will call the transformation (6) Kent Transform (KT). The reasoning of such a transform is the following: a non linear transformation that enhances the separation between 2 distributions which contain values between 0 and 1 is represented by $|\log_{10}(\text{value}^2)|$. This

expression will map values close to 0 above 1 and values above 0.32 below 1. When computing 1 – hyperbolic tangent of this expression, the values from the two original distributions will be more separated than they were initially.

$$\mathrm{KT}(\mathrm{score}) = 1 - \tanh|\log_{10}(\mathrm{score}^2)| \quad (6)$$

We will demonstrate the efficiency of the KT in the experimental results section, but let us first replace the scores of 0.2 and 0.4 in the above formula. Initially, the difference between the impostor score of 0.4 and authentic score of 0.2 is 0.2. After applying the KT we obtain KT(0.4) = 0.33 and KT(0.2) = 0.11 and the difference between the scores is now 0.22, larger by 10%.

When the impostor and authentic scores have values very close to the decision boundary, for example the impostor score is 0.35 and the authentic score is 0.3, then the difference of 0.05 between the 2 scores is increased by 18% to 0.059 when KT is applied. Therefore, the KT is a non-linear transformation which reduces the overlap between the authentic and impostor score distributions of an iris recognition system. KT may as well be applied to any type of biometric system which has the matching scores for authentics and impostors similar to those of a classical iris recognition system.

4 Experimental Results

The database used in our experiments was UBIRISv1 [11] Session 1. This session has 241 users enrolled with one eye. There are 5 colour RGB images for each user. The images were acquired in a semi-controlled environment, by reducing the noise factors, such as reflections, poor illumination or poor focus. The users were at a distance of 20 cm from the acquisition device. However, 10 images out of the total of 1205 are strongly or totally occluded and therefore no useful information can be extracted from them. We ran the experiments on all the images from the dataset, including the occluded ones.

The experimental setup consists of the classical one vs one score generation for all possible combinations between same class images and different class images. The fusion between the scores produced by the 3 algorithms was done by using weighted average. The weights for the 3 algorithms were determined using the first 40 classes via a direct search.

4.1 Using 50 Pixels around the Pupil

In Table 1, the decidability index is reported for all the images of UBIRISv1 Session 1 dataset and the 3 algorithms together with the means and standard deviations (in brackets) of the authentic and impostor distributions. There are 723000 impostor scores and 2410 authentic scores.

The KT is applied to the 8-neighborhood based algorithm and to the 2D Gabor filter based algorithm. The KT is not applied to the GLCM based algorithm because equation (5) which produces the matching scores of this algorithm is similar to KT.

Table 1. Decidability index and distribution means and standard deviations (in brackets) for the 3 algorithms

Algorithm	Authentic mean and std. deviation	Impostor mean and std. deviation	Decidability index
8-neighborhood	0.30 (0.038)	0.39 (0.017)	3.22
8-neighborhood with KT	0.22 (0.043)	0.33 (0.021)	3.31
GLCM	0.10 (0.227)	0.76 (0.336)	2.31
2D Gabor	0.20 (0.064)	0.40 (0.034)	3.92
2D Gabor with KT	0.12 (0.066)	0.34 (0.042)	4.03

In Table 2, the decidability index together with False Reject Rate (FRR) for 2 values of the False Acceptance Rate (FAR) and Equal Error Rate (EER) are reported for the last 201 classes left after the weights were determined using the first 40 classes. The weights obtained for the 2D Gabor with KT, 8-neighborhood with KT and GLCM algorithms are 0.61, 0.31 and 0.08 respectively.

Table 2. Performance measures for the 3 algorithms and fusion approach when 50 pixels around the pupil are used

Algorithm	Decidability index	FRR for FAR=0.01%	FRR for FAR=0.1%	EER
2D Gabor with KT	4.09	10.70 %	7.41 %	3.63 %
8-neighborhood with KT	3.33	22.34 %	11.74 %	3.51 %
GLCM	2.27	99.62 %	97.82 %	15.47 %
Fusion	4.38	11.39 %	7.91 %	3.33 %

From Table 2 may be observed that the GLCM based system performs poor compared to the other 2 algorithms, but when the scores of the 3 algorithms are fused, the decidability index of the best algorithm is increased by approximately 7% and the EER is decreased by approximately 8.2%. We have eliminated the GLCM based algorithm and implemented a weighted average between the other 2 systems, but the decidability index and the EER could only be improved by less than 1%.

4.2 Using 100 Pixels around the Pupil

In Table 3, the decidability index is reported for all the images of the 201 classes used for testing, together with the FRR for given thresholds of the FAR. In this case the optimum weights for 2D Gabor with KT, 8-neighborhood with KT and GLCM algorithms are 0.55, 0.34 and 0.11 respectively.

Table 3. Performance measures for the 3 algorithms and fusion approach when 100 pixels around the pupil are used

Algorithm	Decidability index	FRR for FAR=0.01%	FRR for FAR=0.1%	EER
2D Gabor with KT	4.93	4.42 %	3.38 %	2.45 %
8-neighborhood with KT	3.92	7.51 %	4.12 %	2.45 %
GLCM	3.19	99.58%	98.09 %	8.05 %
Fusion	5.17	10.7 %	4.67 %	2.25 %

The fusion of the 3 algorithms improves the decidability index by approximately 5% and the EER by approximately 8%. However, fusing of the 3 algorithms is not suitable if a low FAR is required for the operation of the iris recognition system.

In Fig. 3, the Receiving Operational Characteristic (ROC) curve is plotted for the 8-neighborhood and 2D Gabor algorithms, together with the ROC curve for the fusion of the 3 algorithms.

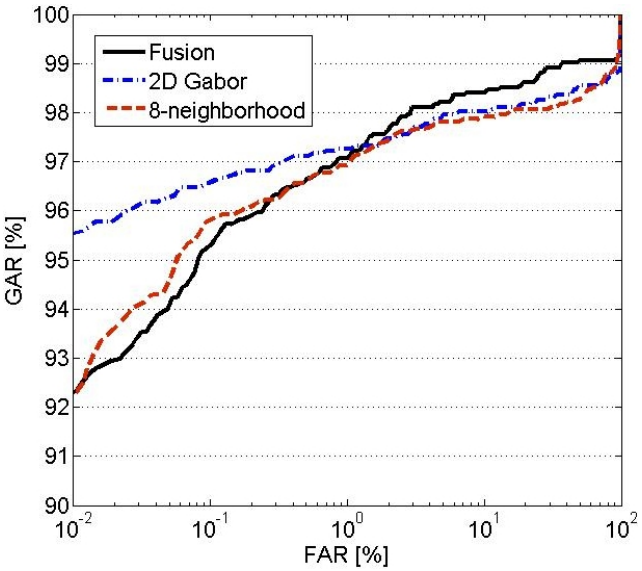

Fig. 3. ROC curve for 8-neighborhood, 2D Gabor and fusion of the 3 algorithms

To observe the improvement brought by using 100 pixels around the pupil over the case when only 50 pixels are used, we plotted in Fig. 4 the authentic and impostor distributions of the fused scores for the 3 algorithms produced on the 201 test classes. The EER when using 100 pixels around the pupil is improved by 32.42% compared to the case when only 50 pixels are used.

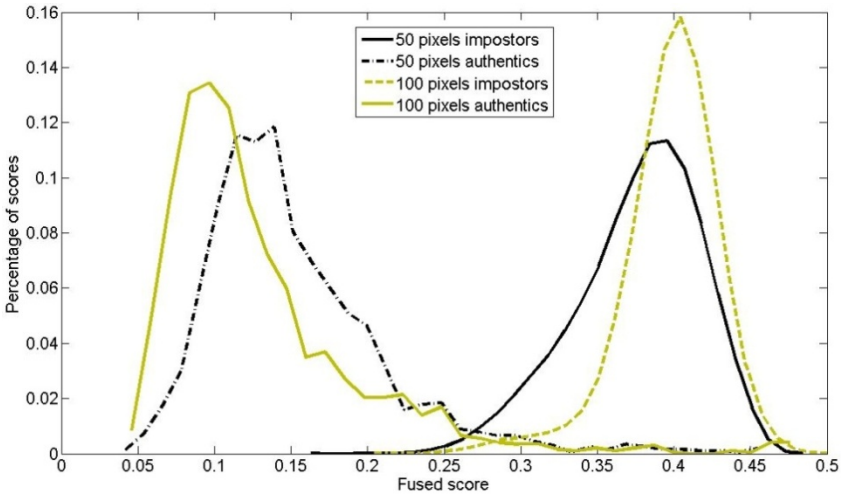

Fig. 4. Authentic and impostor fused score distributions when using 50 pixels and 100 pixels around the pupil

In Table 4. we compare the performance of the proposed fusion approach with that reported in [17] on UBIRISv1 Session 1. As may be observed, our system performs significantly better than the approach proposed in [17].

Table 4. Performance comparison of proposed approach with published works

Method	GAR for FAR = 1%
Hosseini et al [17]	81.70 %
Proposed 2D Gabor algorithm	97.19 %
Proposed 8-neighborhood algorithm	96.98 %
Proposed fusion approach	97.16 %

5 Conclusions

Iris recognition on colour images is a challenging task, becoming an emergent research topic. In this work we propose two iris recognition algorithms, one based on the 8-neighborhood of the iris texture and one based on the GLCM. By fusing the two proposed iris recognition algorithms at the score level with the classical 2D Gabor filter algorithm introduced by Daugman, the EER of the system is improved by approximately 8%.

We introduced a non-linear transformation called Kent Transform, which applied to the matching score of an iris recognition system is increasing the decidability index of the system. We also investigated how the performance of a colour iris recognition

system is affected when using only 50 pixels around the pupil compared to the case when 100 pixels around the pupil are used.

The experimental results show that a multi-algorithmic approach for colour iris recognition is beneficial, even when the accuracy of some component algorithms is significantly poorer compared to the best performing algorithm.

References

1. Daugman, J.G.: High confidence visual recognition of persons by a test of statistical independence. IEEE Transactions on Pattern Analysis and Machine Intelligence 15(11), 1148–1161 (1993)
2. Ma, L., Wang, Y.H., Tan, T.N.: Iris recognition using circular symmetric filters. In: Kasturi, R., Laurendeau, D., Suen, C. (eds.) Proceedings of 16th International Conference on Pattern Recognition, vol. II, pp. 414–417. IEEE Computer Soc., Los Alamitos (2002)
3. Ma, L., Tan, T.N., Wang, Y.H., Zhang, D.X.: Efficient iris recognition by characterizing key local variations. IEEE Transactions on Image Processing 13(6), 739–750 (2004)
4. NIST. National Institute of Standards and Technology (2010), http://www.nist.gov (cited June 30, 2012)
5. Grother, P., Tabassi, E., Quinn, G.W., Salamon, W.: IREX 1 Report - Performance of Iris Recognition Algorithms on Standard Images (2009)
6. Standardization, I.O. f. ISO/IEC 19794-6:2011 (2011), http://www.iso.org/iso/iso_catalogue/catalogue_tc/catalogue_detail.htm?csnumber=50868 (cited May 30, 2012)
7. Proenca, H., Alexandre, L.A.: Toward Covert Iris Biometric Recognition: Experimental Results From the NICE Contests. IEEE Transactions on Information Forensics and Security 7(2), 798–808 (2012)
8. Proenca, H., et al.: The UBIRIS.v2: A Database of Visible Wavelength Iris Images Captured On-the-Move and At-a-Distance. IEEE Transactions on Pattern Analysis and Machine Intelligence 32(8), 1529–1535 (2010)
9. Radu, P., Sirlantzis, K., Howells, W.G.J., Deravi, F., Hoque, S.: Information Fusion for Unconstrained Iris Recognition. International Journal of Hybrid Information Technology 4(4), 1–12 (2011)
10. Radu, P., Sirlantzis, K., Howells, W.G.J., Hoque, S., Deravi, F.: A Versatile Iris Segmentation Algorithm. In: Arslan Bromme, C.B. (ed.) BIOSIG 2011. Kollen Druck+Vwrlag, Darmstadt, pp. 137–151 (2011)
11. Proença, H., Alexandre, L.A.: UBIRIS: A Noisy Iris Image Database. In: Roli, F., Vitulano, S. (eds.) ICIAP 2005. LNCS, vol. 3617, pp. 970–977. Springer, Heidelberg (2005)
12. Vatsa, M., Singh, R., Noore, A.: Improving iris recognition performance using segmentation, quality enhancement, match score fusion, and indexing. IEEE Transactions on Systems Man and Cybernetics Part B-Cybernetics 38(4), 1021–1035 (2008)
13. Nixon, M.S., Aguado, A.S.: Feature Extraction and Image Processing, ed. Newnes 2002: Newness
14. Daugman, J.: How iris recognition works. IEEE Transactions on Circuits and Systems for Video Technology 14(1), 21–30 (2004)

15. Balas, V.E., Motoc, I.M., Barbulescu, A.: Combined Haar-Hilbert and Log-Gabor Based Iris Encoders. In: Balas, V.E., Fodor, J., Varkonyi-Koczy, A. (eds.) New Concepts and Applications in Soft Computing. Studies in Computational Intelligence, vol. 417, pp. 1–26. Springer, Heidelberg (2012)
16. Popescu-Bodorin, N., Balas, V.E.: Comparing Haar-Hilbert and Log-Gabor based iris encoders on Bath Iris Image Database. In: 2010 4th International Workshop on Soft Computing Applications, SOFA (2010)
17. Hosseini, M.S., Araabi, B.N., Soltanian-Zadeh, H.: Pigment Melanin: Pattern for Iris Recognition. IEEE Transactions on Instrumentation and Measurement 59(4), 792–804 (2010)